APPENDIX

Particle image velocimetry (PIV) measurements

PIV is a laser-based non-invasive technique of choice for visualizing and quantifying the full field of fluid movements around moving objects of various sizes and speeds (40). We used the PIV measurement system described by Casas *et al*. (2008) (18). Our experimental setup consisted of two sealed glass boxes (10x6.2x6.2 cm) for the experiments on spheres of 1 mm and 8 mm and a larger box (34x25x17 cm) for experiments on spheres of 30 mm, both seeded with 0.2 μm oil particles. Oil particles (Di-Ethyl-Hexyl-Sebacat, 0.5 L, TPAS, Dresden, Germany) were generated with an aerosol generator (ATM 230, ACIL, Chatou, France). The laser (NewWave Research Solo PIV 2, Nd:YAG, dual-pulsed; Dantec Dynamics A/S, Skovlunde, Denmark) illuminated the flow produced by sphere displacement through the glass box. A laser sheet (width=17 mm, thickness at focus point=50 μm) was operated at low power (3 mJ at 532 nm) to minimize glare. A target area of various sizes (10x8 mm for small spheres of 1 mm and 50x40 mm for larger spheres of 8 mm and 30 mm) was then imaged onto the CCD array of a digital camera (Photron FastCam X1280 PCI 4K) with a macro lens (Nikon, AF Nikkor, 60 mm, f : 2.8). The CCD captured separate image frames (30 fps, 1280x1024 pixels). Once a sequence of two light pulses was recorded, the images were divided into small interrogation areas of 32x32 pixels, which were cross-correlated with flow map software (Flow Manager 4.4. Dantec Dynamics A/S, Skovlunde, Denmark). The inter-frame time was set to 500 μs and the correlation algorithm used yielded valid measurements for particle displacements of down to 0.1 pixels. Observed speeds, and the lowest measurable speed were estimated as described by Casas *et al*. (2008) (18) and Dangles *et al*. (2006) (17).

Testing our implementation of the CFD-FEM numerical scheme for a single translating sphere

CFD-FEM is a very powerful technique, but not without risks and pitfalls. We therefore thoroughly checked our algorithm by (i) experimentally estimating the flow disturbances around a single translating sphere in flow visualization experiments, carried out by PIV, followed by (ii) analytical approximations of the results and (iii) CFD-FEM computations. We used a single translating sphere of various diameters and velocities to cover the whole range of Reynolds numbers corresponding to different flow regimes, as experienced by a running spider.

We experimentally explored five flow regimes (Re=1, 4.2, 16, 154, 577), using combinations of spheres of different diameters (D=1 mm, 8 mm and 30 mm) with various sphere velocities (V=1.7 cm/s, 6.5 cm/s, 25.8 cm/s, 30 cm/s and 31.8 cm/s). These Re numbers correspond to spider speeds of 0.4, 1.8, 6.9, 67 and 250 cm/s. The sphere was mounted on a small rod, which was fixed on a moving controllable piston. The sphere diameter and velocity were constrained to specific values by the availability of sphere diameters and by the way the piston was programmed. Sphere experiments were conducted far from the wall of the measurement box, to avoid ground and wall effects. We used PIV to determine the flow velocities in a plane crossing the center of the moving spheres. The velocity profiles were extracted in the direction of sphere displacement (See Figure in the electronic appendix).

We fitted two analytical approximations of the Navier-Stokes equation, representing two extreme cases of flow regimes, to the data. For the lowest flow regime, the analytical approximation of the full Navier-Stokes equation is known as the Stokes approximation. The flow velocity components according to Stokes are:

$$u_r = U\cos\theta\left(\frac{3}{2}\frac{a}{r} - \frac{1}{2}\frac{a^3}{r^3}\right)$$

$$u_\theta = Usin\theta\left(\frac{3}{4}\frac{a}{r} + \frac{1}{4}\frac{a^3}{r^3}\right)$$

where U is the sphere velocity, θ is the angle with respect to the direction of movement of the sphere, *a* is the radius of the sphere and *r* is the distance from the sphere center. In the direction of sphere displacement (where θ =0, cos θ=1 and sin θ=0), these components become:

$$u_r = U\left(\frac{3}{2}\frac{a}{r} - \frac{1}{2}\frac{a^3}{r^3}\right)$$

$$u_\theta = 0$$

For the high-flow regime, the analytical approximation of the full Navier-Stokes equation is known as the potential flow approximation. The flow velocity components in the direction of sphere displacement (at θ =0, cosθ=1 and sinθ=0) are, according to potential flow theory:

$$u_r = U\left(\frac{a^3}{r^3}\right)$$

$$u_\theta = 0$$

The Stokes approximation to experimental PIV measurements was found to be valid only for *Re* numbers of one or below (Figure in the electronic appendix). The potential flow approximation was valid at high *Re* numbers but remained unsatisfactory for the observed speed of spider locomotion, even at the highest (40 cm/s). Both analytical models were found to be poor approximations of the flow for the whole range of speeds used by attacking spiders.

We then compared the CFD-FEM implementation of a translating sphere, using the same parameters as described in the main text, with the experimental data and analytical solutions. The figure in the electronic appendix shows that the CFD-FEM implementation fitted the experimental data very well, and this was confirmed by analytical approximations, where valid. We used the same computational parameters as for simulations of three

translating spheres for a running spider, as explained in the main text, except for the distance to the ground and the simulation volume (reflecting the dimensions of the PIV measurement boxes). We modeled flow disturbances around a quarter of the sphere only, because there was no ground effect in these CFD simulations. We assumed horizontal and vertical flow symmetry, by defining an axis centered on the sphere and oriented in the direction of its displacement. The boundary conditions of the simulation volume were chosen so as to stay as close as possible to the PIV measurements. The velocity at the surface of the sphere was therefore set to the inlet velocity, whereas the upstream and downstream boundaries of the simulation volume were defined as open boundaries with normal stress.

LEGEND FIGURE APPENDIX. Flow velocities upstream from a translating sphere as function of the speed of translation for various *Re* numbers (left) and a full-field 3D view of the finite element model (right). Single-point measurements of flow velocities were obtained by PIV (empty circles, only one measurement per velocity). In each panel, we also present the velocities obtained from CFD-FEM computations (full dots), predicted according to the Stokes (upper green line) and potential flow (lower red line) analytical approximations. Flow velocities and distances from the sphere are normalized, to harmonize data obtained for different sphere diameters and speeds. In the 3D representation, the flow amplitudes are shown in color and the vectors represent the amplitude and direction of flow.

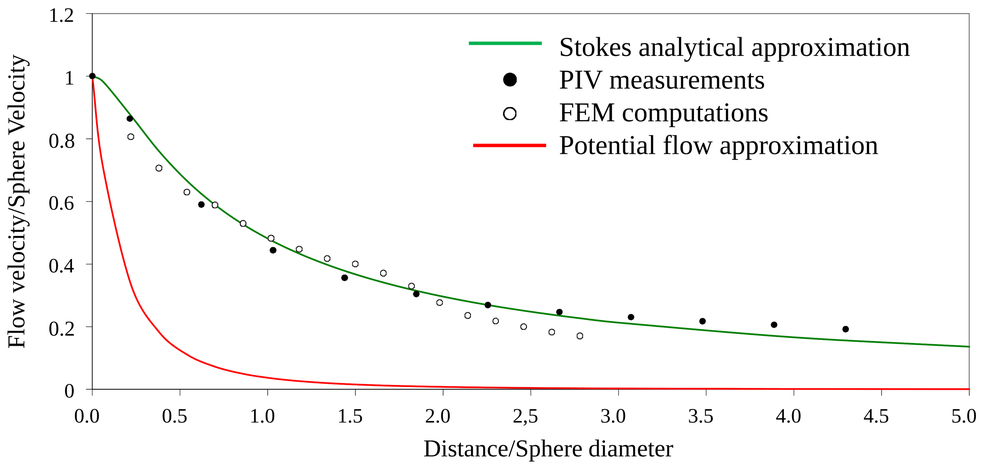

Re=1

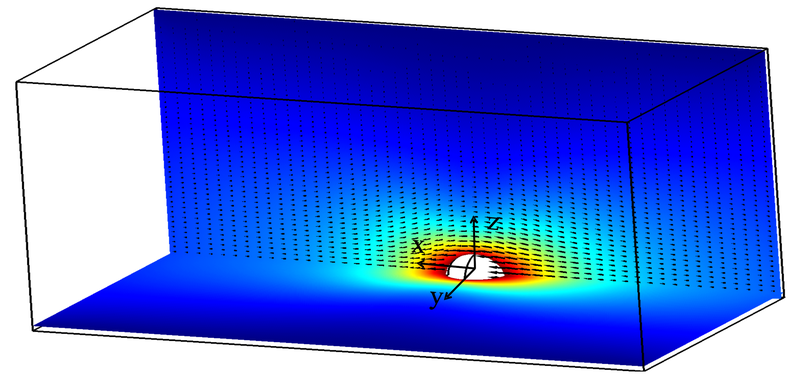

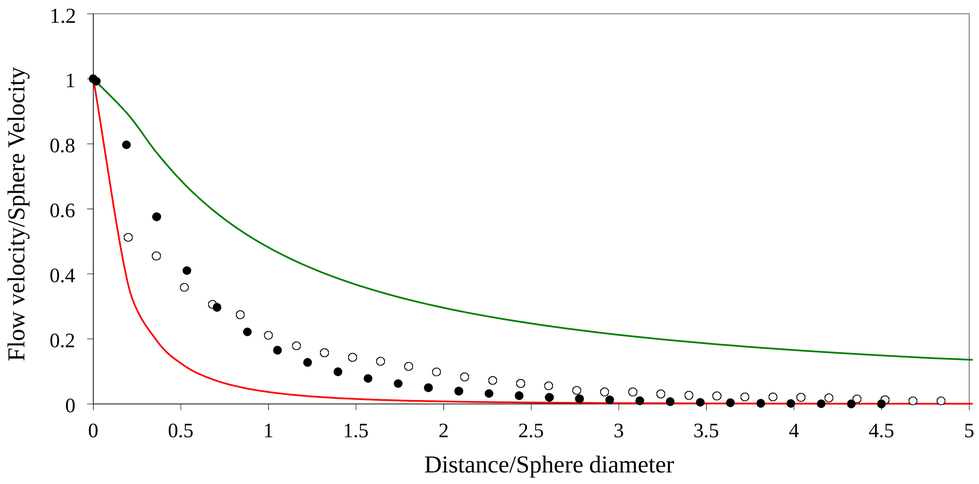

Re=4.2

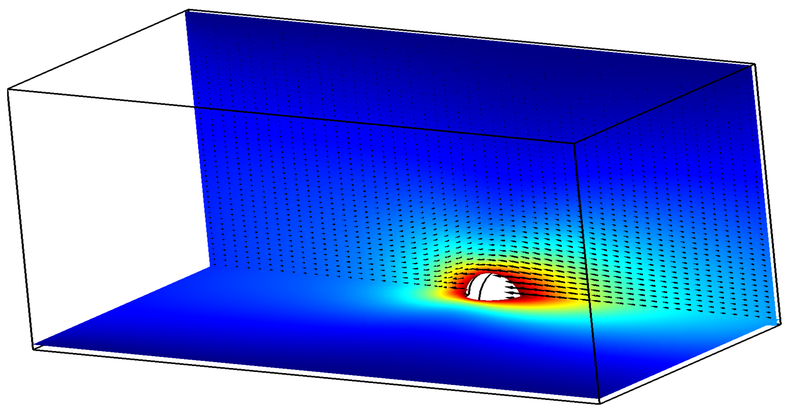

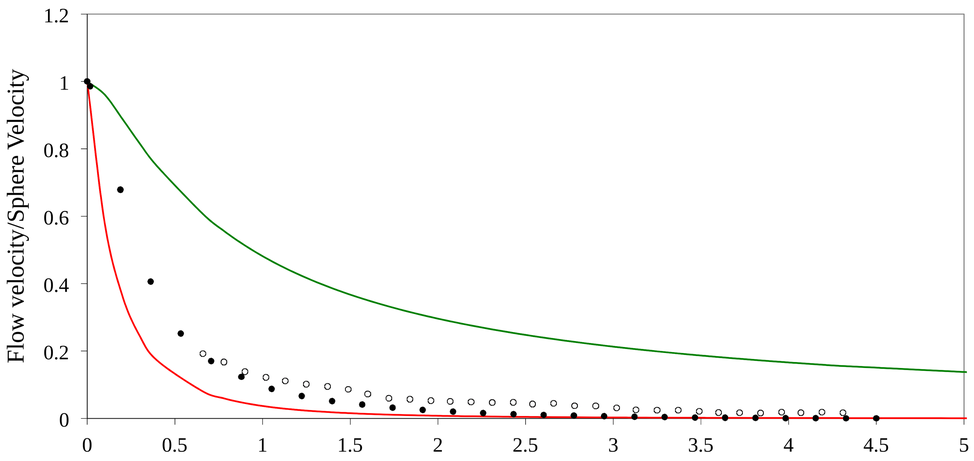

Re=16

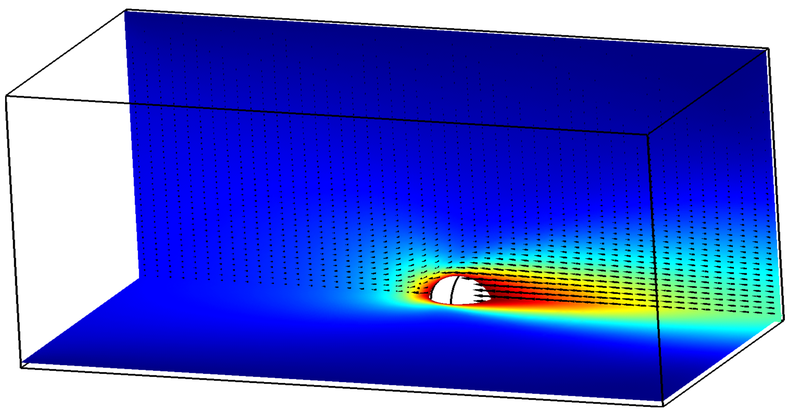

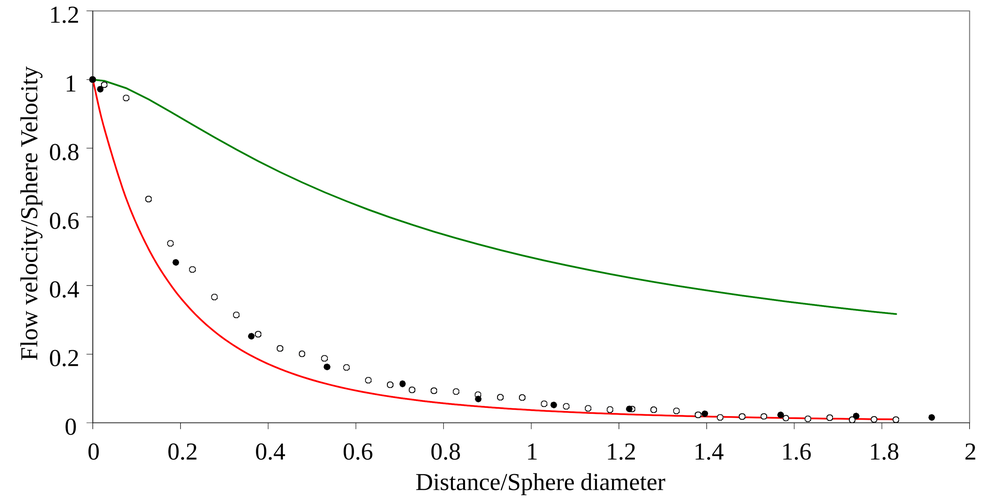

Re=154

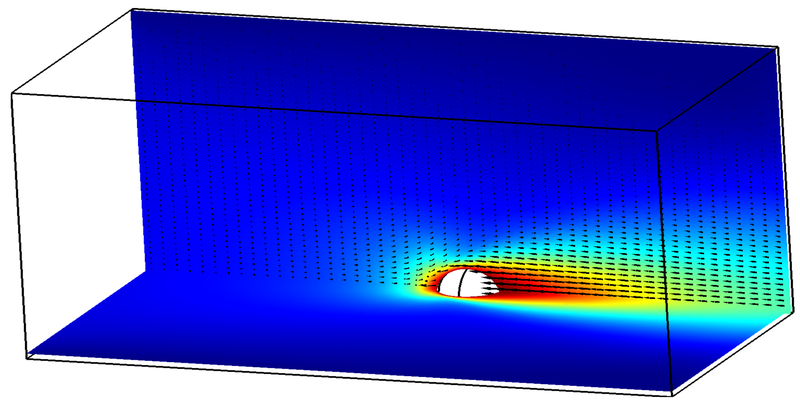

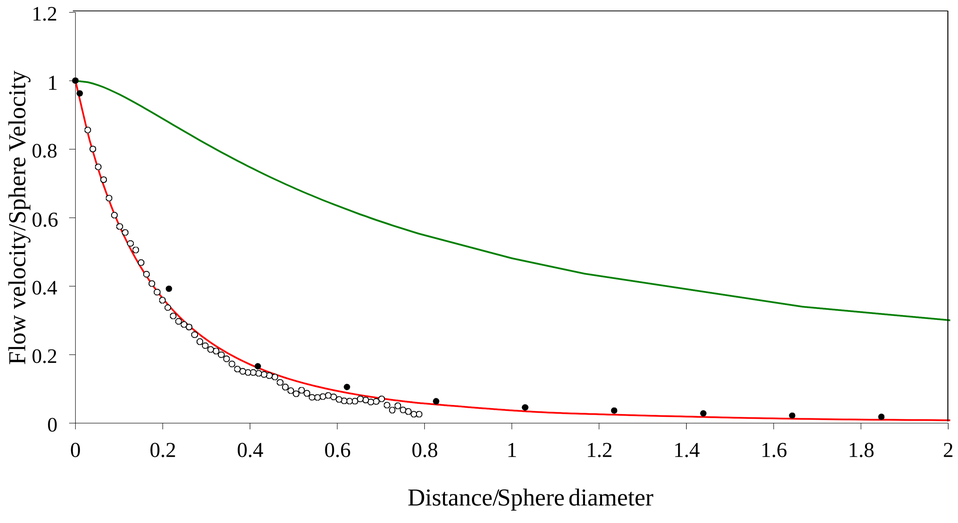

Re=577

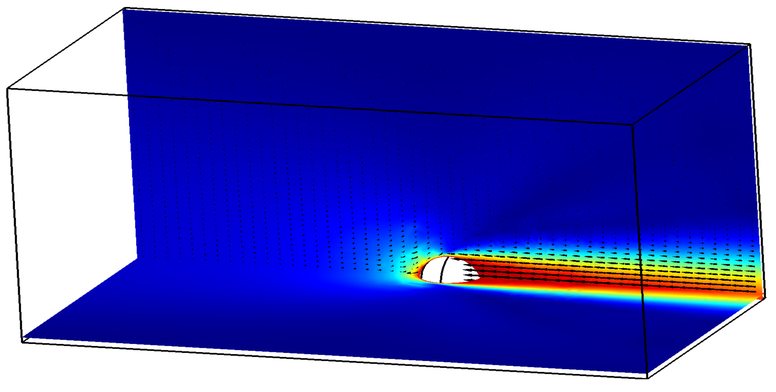

Flow velocity/Sphere velocity

0 0.5 1